ELSEVIER

S0032-3861(96)00555-1

Polymer Vol. 38 No. 3, pp. 677–688, 1997

0032-3861/97/$17.00 + 0.00

Domain structures in magnetically orientated liquid crystalline polymers

Hazel E. Assender and Alan H. Windle*
Department of Materials Science & Metallurgy, University of Cambridge, Pembroke Street, Cambridge CB2 3QZ, UK
(Received 10 November 1995; revised 3 May 1996)

The microstructure of a thermotropic liquid crystalline polymer orientated in a magnetic field is observed to consist of tessellated domains of high alignment bounded by inversion walls. The presence of these walls limits the degree of global orientation achievable with a given field strength, and leads to the rapid loss of orientation on removal of the field. A supra-molecular lattice model for simulating textures in liquid crystals is utilized to simulate the effect of an applied field on a nematic, and the role of disclinations in the formation and destruction of the network of walls is considered. © 1997 Elsevier Science Ltd. All rights reserved.

(Keywords: liquid crystalline polymer; domains; magnetic ordering)

INTRODUCTION

When main-chain thermotropic liquid crystalline polymers are exposed to a magnetic field while held in the liquid crystalline phase (above ~300°C), the molecules are observed to reorientate† along the field direction because of their diamagnetic anisotropy. The results presented in this paper were obtained using a specially synthesized random copolymer of hydroxybenzoic and hydroxynaphthoic acids in the ratio 3:1 and of molecular weight 5000 (hereafter referred to as BN)‡.

Previous measurements of the kinetics of the orientation process[1] have indicated that the rate of orientation is initially high, but decreases until a maximum degree of orientation is achieved which is less than perfect. The rate increases with the square of the strength of the applied field. Removal of the field while the sample is held in the nematic phase leads to a 'relaxation' of the orientation[2] which decays rapidly to zero[3,4].

Both the limitation of the degree of orientation under the applied field, and the loss of this orientation on the removal of the field may be explained in terms of residual elastic defects, such as inversion walls, that are 'trapped' in the material by the field. As the field strength is increased, the defects are more tightly compressed, and the global orientation is increased. If the field is removed (while the material is held in the liquid crystalline phase such that the molecules are still mobile), the compressed elastic deformations associated with the defects rapidly 'spring back' to occupy more and more of the sample volume and thus decrease the orientation. The development of microstructure has been studied by Anwer and Windle[5]; this paper extends this work as a detailed study of domain walls and their organization into networks.

OBSERVATIONS OF MICROSTRUCTURE

Extruded pellets of the samples were ground to a fine powder (~50 μm), melted and quenched. Scanning electron micrographs (SEMs) of samples prepared in the absence of a field showed local molecular alignment forming a randomly orientated texture on a scale of about 30 μm. The overall orientation of such samples, as measured by wide angle X-ray scattering (WAXS), was zero.

On orientation in the melt under an applied magnetic field, a characteristic texture was observed using the methods of both transmission optical microscopy (TOM) of thinly ground sections and scanning electron microscopy (SEM) of fractured samples. As reported before[5], the texture consisted of very highly aligned regions with the molecular direction lying in the field direction, bounded by 'walls' of misorientation. These regions have been described as 'domains', as generally defined[6]. They were elongated in the field direction: a field of 1.12 Telsa for 30 min giving dimensions of about 300 μm long (in the direction of the field axis) by 100 μm wide. The optical contrast observed across the domain walls was consistent with the structure of inversion walls as described by Nehring and Saupe[7].

Examples of the two limiting types of inversion wall in a field-orientated liquid crystalline sample, the splay/bend type and the twist type, are shown in *Figures 1a* and *1b*. The splay/bend and twist wall structures are analogous to 180° Néel and Bloch walls respectively, as understood for ferromagnetic materials. *Figure 2a* shows the domain texture of a field-orientated sample. The scale of the domains is the same as for those observed optically[5] and the organization of the walls may be traced out, as shown in *Figure 2b*.

* To whom correspondence should be addressed
† The *local* parallelism of the directors in the liquid crystal is referred to here as 'alignment'. The direction of this alignment may vary across the sample. The 'orientation' of a sample is the degree to which the directors lie parallel to some fixed direction (e.g. the direction of the applied field) on a global scale. Thus, for example, the areas of alignment, initially in random directions may be reorientated to lie in a single direction on application of an external field
‡ Supplied by Hoechst-Celanese Corporation

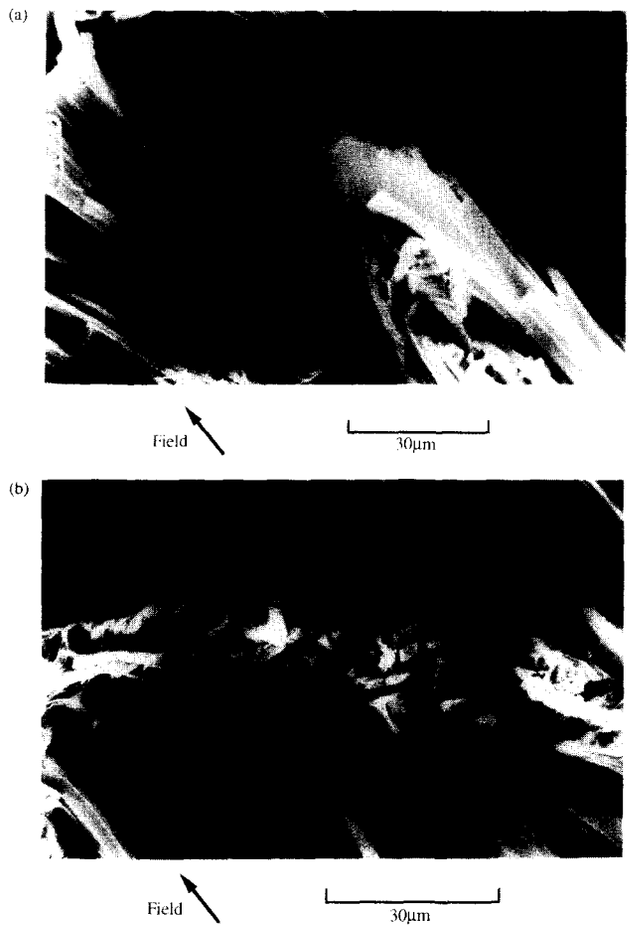

Figure 1 SEMs of fracture surfaces of BN, molecular weight 5000 held for 30 min at 300°C in a field of 1.12 T. (a) An example of a splay-bend wall. The directors rotate about an axis perpendicular to the micrograph, in the plane of the wall. (b) A twist wall. In this case the wall lies in the plane of the micrograph, and the rotation axis of the directors lies perpendicular to this. The fractured ends show how successive layers of polymer lie at different angles to the field direction

The walls meet at triple junctions, giving a continuous network of tessellating domains. Within such a network, the wall area, which is associated with distortion of the liquid crystal, should be minimized, and Thomson[8], working on the shapes of bubbles contained in foams, has predicted that such shapes would be fourteen sided figures—tetrakaidecahedrons. It is also known from the pioneering work of Plateau[9] that only three walls can meet to form lines and that only four such lines can meet at a point. More recent theories[10] can predict lower energy structures using combinations of domains of different sizes, but experimentally all the domains observed in the orientated liquid crystalline polymer specimens appear to be of equal size. Thus the observed domain structure may be thought of as a network of interlocking triple point lines with the domain walls defining the planes between them.

It has been observed[3,4] that the structure which develops as the orientation relaxes after the field is removed is coarser than that in samples held for the same period in the absence of a field.

THE EFFECT OF A MAGNETIC FIELD ON A DOMAIN WALL

Under the influence of an aligning field, it is expected that domain walls would become narrower, increasing

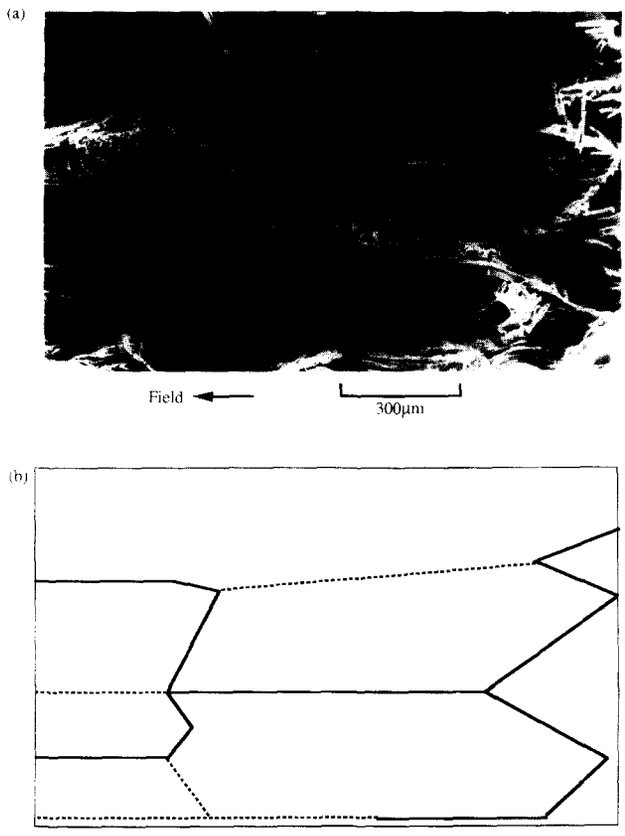

Figure 2 (a) SEM of a fracture surface of BN, $M_w = 5000$, treated for 30 min in a field of 1.12 T at 300°C. The domain walls are outlined in (b). Note the high level of orientation within the domains, and the wall structures bounding them

the volume of the domains and thus bringing more directors towards the field direction. This development is limited when the increased elastic energy associated with the narrowing walls offsets the gains associated with the increased orientation to the field within the domains. The equilibrium wall width as a function of the applied field strength has been measured for two similar polymers[5,11] and the results are reproduced in *Figure 3*. The angle of the director to the field direction varies across the wall according to the relation[12]

$$\frac{\chi_a B^2}{\mu_0}\sin\theta\cos\theta - K\frac{d^2\theta}{dx^2} = 0 \qquad (1)$$

where K is the elastic constant (assuming all distortion types to have the same elastic constant), μ_0 is the permeability of free space and χ_a is the anisotropy in the diamagnetic susceptibility. This has the solution[11]

$$x = \pm\left(\frac{\mu_0 K}{\chi_a B^2}\right)^{1/2}\ln\left(\tan\frac{\theta}{2}\right) \qquad (2)$$

and so the director only becomes exactly parallel to the field at infinite distance from the wall centre. Defining the wall limits as the planes on which the directors have orientated to within, say, 5° of the field direction, the measured widths are seen to depend on the field strength as shown in *Figure 3*. Furthermore the width of the wall, W, can now be expressed as

$$W \approx \frac{6}{B}\left(\frac{\mu_0 K}{\chi_a}\right)^{1/2} \qquad (3)$$

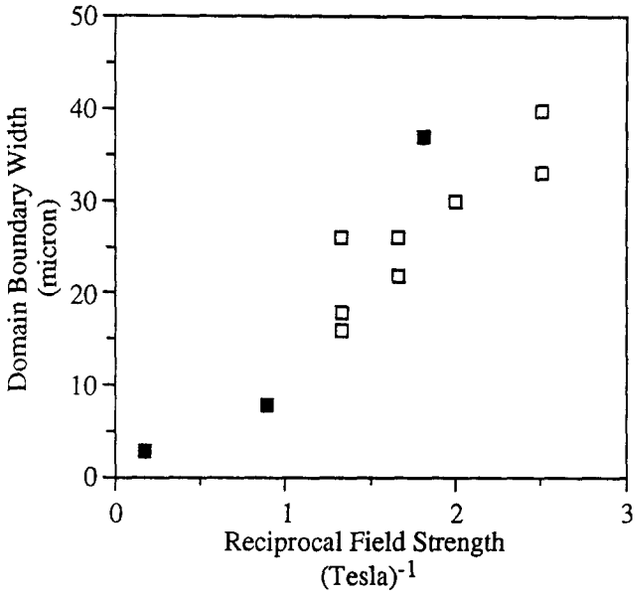

Figure 3 The relationship between the domain boundary width and the reciprocal of the applied field strength for BN (■) and for a similar main-chain thermotropic polymer with flexible sequences in the backbone (□)[11]. Reproduced from ref. 5

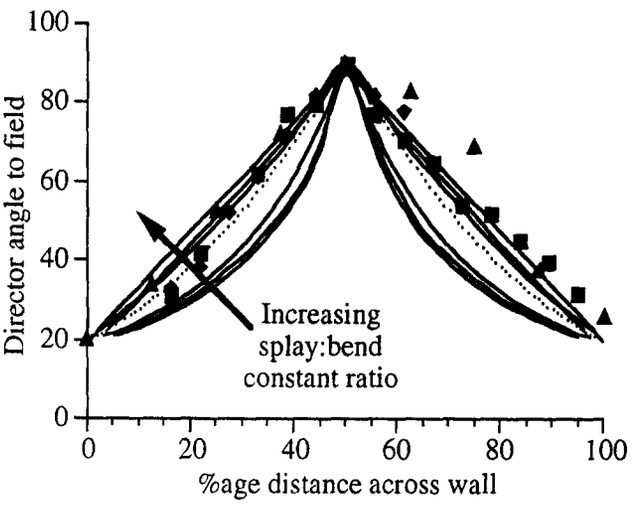

Figure 4 The shape of a domain boundary as given by the variation in angle of the director as the boundary is traversed for different ratios of the elastic constants for the splay and bend distortions (K_1 and K_3 respectively). The ratios from the inner to the outer curves are: $K_1/K_3 = 1/10$, 1/2, 3/4, 1 (dashed line), 4/3, 2, 10. The dark points are angles of directors as measured from electron micrographs—the different symbol shapes each representing one of the three different micrographs

which enables the ratio K/χ_a to be determined from a linear fit to the data. Using a diamagnetic anisotropy of $\chi_a = 1.1 \times 10^{-8}$ which may be typical of main-chain liquid crystalline polymer systems[13,14], the data of *Figure 3* give a value of 7×10^{-14} N for the elastic constant, K. Bearing in mind that these data are from two different polymers which may have different values of χ_a (the gradient of the data from the more flexible polymer alone was estimated to be lower in the original publication[11]), and that the elastic constants for the splay and bend distortions are not expected to be equal, the value predicted for the elastic constant is nevertheless in the expected range.

Equation (2) is a function whose shape is independent of the field strength, that is the plot of the angle of the director to the field axis against the fractional distance across the wall width (defining the edges of the wall as some arbitrary angle, as above) will be the same for all field strengths. The shape of a splay/bend wall will, however, be dependent on the relative sizes of the splay and bend constants. Meyer[15] demonstrated that for polymer liquid crystals the splay constant (K_1) increases with molecular weight because to maintain constant density in a region of divergence requires a segregation of chain ends which invokes an entropy penalty. K_2 and K_3 do not continue to increase with molecular weight as they reach a limit which depends upon the persistence length rather than the chain length[16]. Experimental values for the elastic constants in a copolyesteramide have been reported by de'Nève *et al.*[17] as around

$$K_1 = 10^{-8}\,\text{N}$$
$$K_2 = 10^{-10}\,\text{N}$$
$$K_3 = 10^{-9}\,\text{N}$$

for a polymer with molecular weight 20 000. The polymer measured in this case is, however, of a length much closer to the persistence length (with molecular weight 5000), and so the splay constant is perhaps expected to be not so much greater than the bend constant.

Equation (1) may be extended for the case of $K_1 \neq N_3$[12]

$$\frac{\chi_a B^2}{\mu_0}\sin\theta\cos\theta - K_1\cos\theta\frac{d}{dx}\left(\cos\theta\frac{d\theta}{dx}\right) - K_3\sin\theta\frac{d}{dx}\left(\sin\theta\frac{d\theta}{dx}\right) = 0 \quad (4)$$

Hence

$$\frac{d^2\theta}{dx^2} = \frac{\sin\theta\cos\theta\left(\frac{\mu_0 K}{\chi_a B^2} - (R-1)\frac{d\theta}{dx}\right)}{(R-1)\sin^2\theta + 1} \quad (5)$$

where R is the ratio of the splay/bend elastic constants, so: $K_1 = RK_3 = K$. By solving this analytically, one may predict the shape of the wall for different ratios of the splay and bend constants as shown by the continuous curves of *Figure 4*. The change in shape is independent of the ratio of K to B, and the shape is not greatly altered by increasing the ratio of the elastic constants beyond about 10 in either direction. Basically, for $K_1 > K_3$ the orientation changes linearly with position across the wall, while for $K_1 < K_3$ the orientation changes much more steeply with position on approaching the centre. The angular change in the director across the wall has been measured from SEMs of three walls in magnetically orientated samples. The data, plotted in *Figure 4*, are to the outer side (high splay side) of the $K_1 = K_3$ curve, although it is difficult to determine a precise ratio.

THE LATTICE MODEL

A lattice model, developed to simulate the textures observed in liquid crystals[18–21], may be applied to the case of field orientated samples. A cubic array of vectors, each representing an area of good local orientation (*Figure 5*), is set up either in initially random orientations or to represent a particular initial texture. Each vector is considered to represent a local *director* (the average orientation of many mesogenic units) and thus the model

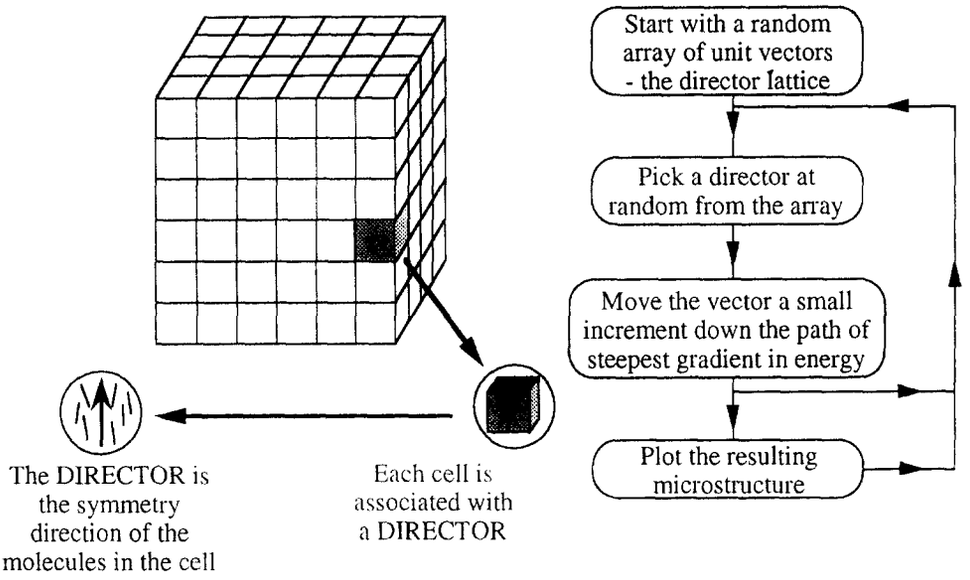

Figure 5 The supramolecular lattice model. Each cell is characterized by a director, and is taken to be much larger than molecular dimensions. On the right the model's algorithm is outlined. Each cell is visited at random, and the orientation of its vector changed on a path which will reduce its energy with respect to the orientation of the directors of the six nearest neighbour cells

is on the supra-molecular scale. These local directors have an energy associated with their misalignment in relation to their six nearest neighbours. The energy is given by the expression

$$E = \sum_{i=1}^{6} \sin^2(\theta_i - \phi) \qquad (6)$$

where $(\theta_i - \phi)$ is the angle between the vector under consideration and its ith neighbour.

The directors are visited at random in the model and moved through a small angle down the path of steepest energy gradient: the algorithm is illustrated in *Figure 5*.

The effect of a magnetic field may easily be included into the model algorithm by the introduction of a seventh term to the energy equation. The field will have a similar aligning effect as a neighbouring vector: when the director lies parallel to the field the energy is a minimum, and when it lies perpendicular, it is a maximum. The energy expression becomes

$$E = F \sin^2(\theta_f - \phi) + \sum_{i=1}^{6} \sin^2(\theta_i - \phi) \qquad (7)$$

where $(\theta_f - \phi)$ is the angle between the vector and the field direction and F is the field coefficient—giving the relative energies of the elastic distortions and misalignment to the applied field.

The supra-molecular lattice model has been utilized to simulate the effect of the inversion walls narrowing under the influence of an applied field. *Figure 6* shows results of the simulations of a field applied to a splay–bend wall. The initial conditions (*Figure 6a*) define a wall in the yz plane in which there is a constant rotation of the directors as the wall is traversed: all directors lying in the xy plane. The field direction lies in the y axis. The distortion energy of all vectors is the same, but those vectors at the centre of the wall have the maximum misalignment to the field direction and hence the maximum overall energy. The overall energy profile is shown on the right of the diagram.

As the simulation progresses, the directors far from the wall turn towards the field direction, compressing the

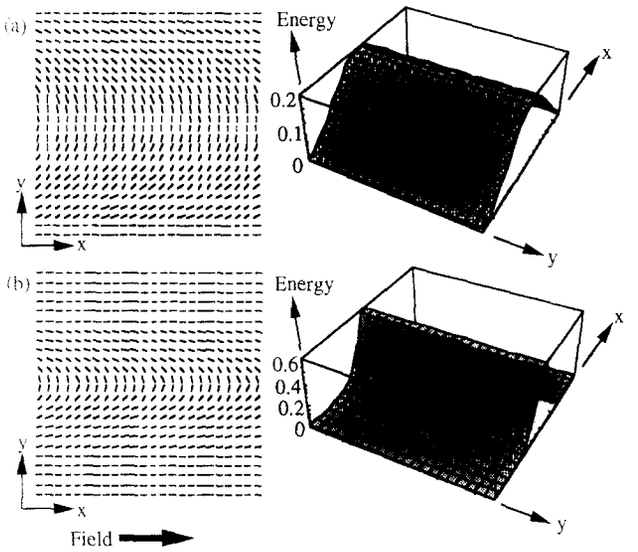

Figure 6 Simulation of the effect of a field on a splay–bend wall. The initial conditions (a) define a wall, shown as a director map of one layer through the lattice on the left, and the energy profile on the right. (b) The equilibrium structure after applying a field of coefficient $F = 0.2$. The distortion is now confined to a narrower width

wall, and increasing the elastic distortion at the centre. *Figure 6b* shows the equilibrium texture for the field strength applied (the simulation having been run for many thousands of iterations after the directors were seen to stop moving). The wall has narrowed to an equilibrium width and has been stabilized by the field. If the effect of a field were to be removed from the simulation after reaching equilibrium with the field applied, the wall would widen once more: the enhanced alignment induced by the loss of the field. The strength of the field applied determines the equilibrium width of the wall. *Figure 7* shows the relation between F and the equilibrium wall width as measured from the lattice simulations. The width of the wall is defined as the number of vectors between the points at which the director lies at greater than 10°, 30° and 50° from the field direction. The simulations were performed on a lattice

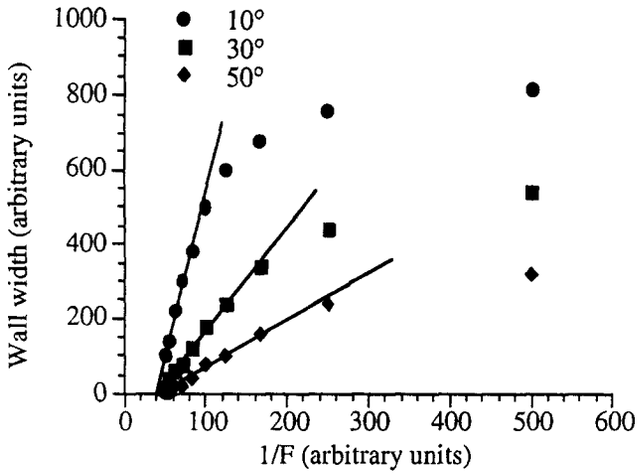

Figure 7 Equilibrium boundary width simulated with various field strength coefficients. The width is defined as the number of lattice vectors between either side of the wall which lie at a greater than 10°, 30° or 50° angle to the field direction

with 1000 vectors in the x direction (across the wall). The central portion of the width vs $1/F$ graph is linear, but at low field strengths (towards the right of the diagram) the wall width is of the order of the model size and thus the vectors 'feel' the model edges (they are influenced by fewer neighbours and therefore tend to lie towards the field direction), limiting the wall width, so the width does not increase linearly as expected. At high field strengths (towards the left of *Figure 7*) the data do not indicate a straight line through the origin, as expected (at infinite field strength the boundary has no width), because the boundary has become very compressed at high fields, and neighbouring vectors take up relatively high angles to one another on the lattice. Equation (1) is derived from elastic energy expressions assuming the angles between successive directors is small. The energy expression used in the model (equation (6)) accommodates high angles, but results in an offset in the data for high F where equation (1) no longer holds. The offset is the same whatever angle is chosen to define the edge of the wall, and whatever the lattice size. Measurement of the gradient of the linear part of this graph cannot directly lead to a relation between the field strength and the elastic constants of the material as both sets of units are arbitrary, but the gradient increases as the angle defining the wall edge decreases, as predicted from equation (2). Note that the energy of interaction of the field with a director is independent of the volume over which that director represents orientation, whereas the energy of elastic interactions between neighbouring vectors does depend upon the distance between them, and so the ratio between F and the elastic constant is dependent upon the scale of the model.

DEFINITION OF DOMAIN WALLS AND THEIR INTERACTION

The nature of a wall may be defined in a similar way to a disclination line[21], that is by a rotation vector which defines the axis of the 180° rotation of the director as the wall is traversed. The splay/bend or twist character of the wall is determined by the angle of this rotation vector to the plane normal of the wall. If the rotation vector and the plane normal are parallel, the wall is of twist character; if they are perpendicular it is based on

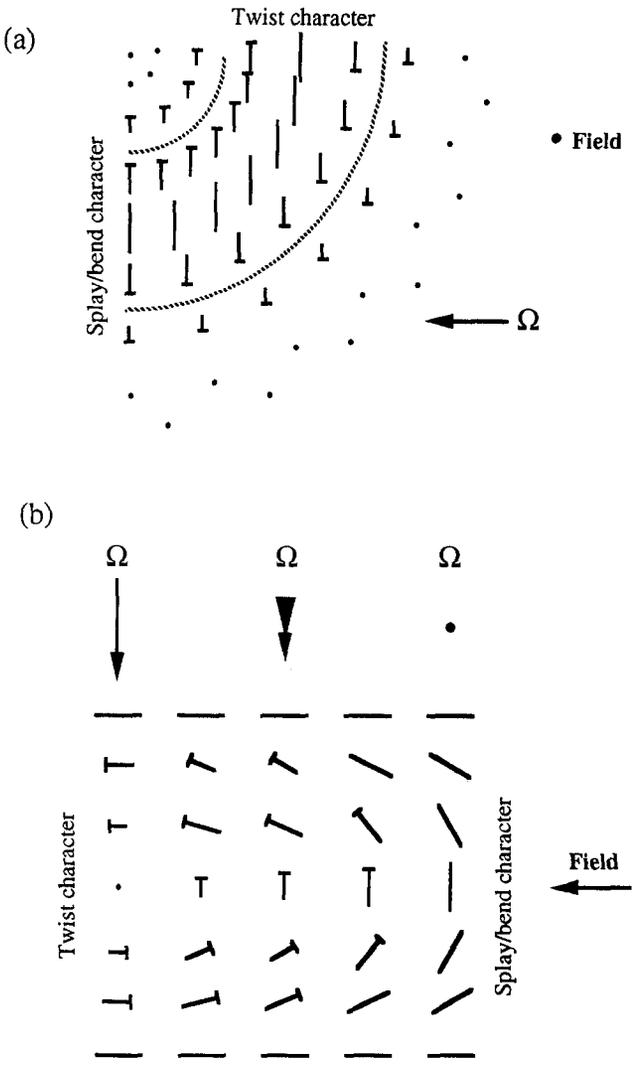

Figure 8 Inversion walls changing nature between splay/bend and twist types. (a) The rotation vector is constant and the direction of the wall changes. (b) The wall direction remains constant, but the rotation vector smoothly rotates such that the wall nature is changed. 'Pin-head' notation is used throughout this paper to indicate vectors lying out of the plane of the page: the point of the 'pin' is directed out of the paper, towards the reader

splay/bend distortions. For the case that the orientations of the directors far from the wall are along the field axis, then at the centre of the wall the directors will be exactly perpendicular to the field. Hence any wall induced by an applied field will have its rotation vector perpendicular to the field direction. It follows that for a wall lying perpendicular to the field, its normal (parallel to the field) is necessarily perpendicular to the rotation vector, and thus the wall must be of splay/bend character. On the other hand, a wall parallel to the field can be either splay/bend or twist character. *Figure 8* illustrates that the nature of a wall may change either as a result of the wall changing direction with respect to a stationary rotation vector, as shown in *Figure 8a*, or as a result of the rotation vector smoothly changing direction along a planar wall, as in *Figure 8b**.

* Kléman[22] showed that the nature of a 180° wall in a ferromagnet may be changed between Bloch and Néel type by the inclusion of a disclination: the disclination being two half strength disclination lines with perpendicular rotation axes superimposed to one another, resulting in no core singularity

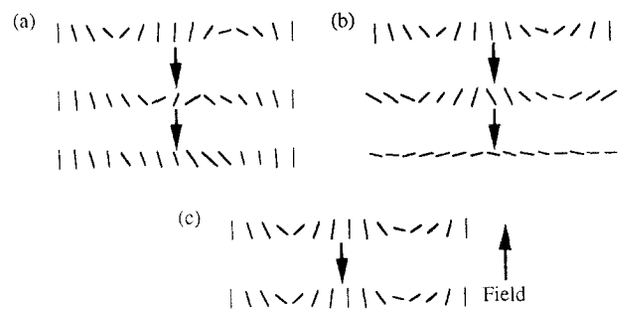

Figure 9 The interactions of the domain walls. (a) Walls of the opposite sign attract one another and annihilate to form a well aligned nematic. Walls of the same sign repel and may open out to form an undistorted director field (b), or be contained by boundary conditions or an external field, stabilizing the walls (c)

Domain walls of opposite sign or 'handedness' will be attracted to one another and can annihilate to form a monodomain of liquid crystal, as is illustrated in *Figure 9a*. If the walls are of the same sign, the force is repulsive, and the walls repel one another. If the walls are not contained, either by boundary conditions or by the application of an external field, the walls will widen without bound to give a monodomain as shown in *Figure 9b*, but if they are constrained by a field, and of the same sign they are stabilized (*Figure 9c*).

DISCLINATION/WALL INTERACTIONS

As both a disclination and an inversion wall may be defined by a vector describing the axis of the 180° rotation of the director, so it is the summation of these vectors that determines the effect of combining these defect types. In the case of disclinations, the singularities will attract and annihilate to form undistorted material if the rotation vectors of the disclinations are antiparallel. In a similar way, two walls of opposite 'handedness' (i.e. with their rotation vectors antiparallel) will attract one another and annihilate (as discussed above) and, as for disclinations, two walls with parallel rotation vectors (the same 'handedness') will repel one another. Similarly the rotation vector of a wall and of a disclination can also be summed in this way, and thus a disclination line will define the limit of a wall with an antiparallel rotation vector. Examples of disclinations which terminate walls are depicted in *Figure 10*.

When an external field is applied to a disclination line in which the directors to one side of the disclination line are parallel to the field direction, the disclination line will tend to move so as to increase the volume of aligned material. In general, therefore, disclination lines will move in a preferred direction in response to an applied field. However, for the special case of a disclination with a rotation vector parallel to the field direction, all the surrounding directors lie perpendicular to the field direction, and so the disclination will not be moved by the action of the field.

We have shown that a disclination line defines the limit of a wall with the same rotation vector. If a disclination loop (a type I loop[21], with a constant rotation vector) were to form, therefore, within an area of undistorted liquid crystal, it would enclose an area of wall with the same rotation axis as the disclination (*Figure 11a*). Conversely, were a disclination loop to form within an

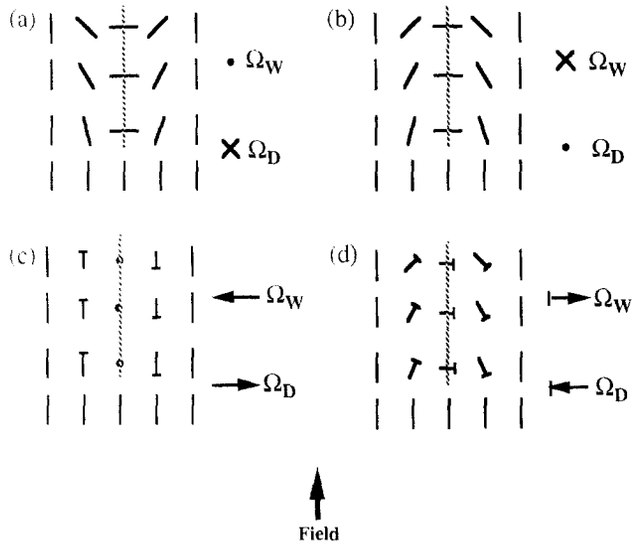

Figure 10 An inversion wall will be terminated by a disclination with the same rotation vector (Ω_D) as that of the wall (Ω_W). Examples are shown here for (a) an $s = -1/2$ wedge disclination terminating a splay/bend wall, (b) an $s = +1/2$ wedge disclination terminating a splay/bend wall, (c) a twist disclination terminating a twist wall, and (d) a mixed-type disclination terminating a wall involving both splay/bend and twist distortions (in this case the rotation vectors are no longer in the plane of the page). In all cases the field direction is vertical, and the wall (above the disclination) changed to a monodomain (below the disclination)

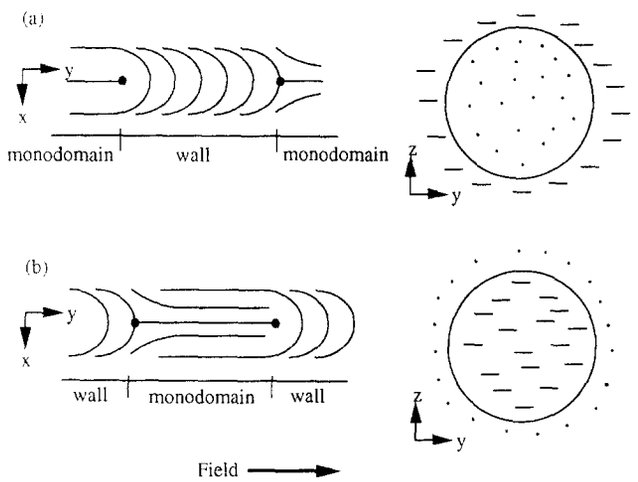

Figure 11 (a) A disclination loop in a monodomain surrounds an area of inversion wall. (b) A disclination loop within an inversion wall surrounds an area of undistorted liquid crystal within the wall

area of domain wall and the rotation vector of the loop and the wall were parallel, the loop would enclose an area with no inversion wall (*Figure 11b*). The question should be addressed as to whether in each of these cases the disclination loop will grow or shrink in response to the distortion energies of the wall and disclination, thus forming either a larger area of wall or of undistorted liquid crystal.

An expression for the energy of a domain wall per unit area may be derived by considering the angle ϕ of the director rotating in a plane perpendicular to the rotation axis of the wall. Hence:

$$\int_0^W \nabla\phi dx = \pi \tag{8}$$

where W is the width of the wall. Assuming that $\nabla\phi$ is

constant across the whole wall width, then

$$\nabla\phi = \frac{\pi}{W} \tag{9}$$

thus the elastic energy of a unit area of wall, if all distortions have the same elastic constant, K, is

$$E_{\text{wall}} = \int_0^W \tfrac{1}{2}K(\nabla\phi)^2 dx = \frac{K\pi^2}{2W} \tag{10}$$

The energy associated with a disclination loop (if interactions of the disclination line with itself are ignored) is given by[21]

$$E_{\text{loop}} = 2\pi K s^2 R\left(\ln\left(\frac{R}{r_c}\right) + \frac{1}{2}\right) \tag{11}$$

where R is the radius of the loop and r_c the radius of the core of the disclination of strength s.

A type I disclination loop set within an area of undistorted liquid crystal will enclose a wall (*Figure 11a*), and, not surprisingly, will tend to collapse, decreasing both the length of the loop and the area of wall. However, for a type I loop which encloses a mono-domain within a wall (*Figure 11b*), the energy of the system is given by the expression:

$$E_{\text{total}} = E_{\text{wall}} + \frac{\pi^2 K}{2}\left(R\left(\ln\left(\frac{R}{r_c}\right) + \frac{1}{2}\right) - \frac{\pi R^2}{W}\right) \tag{12}$$

Figure 12 indicates how the energy of the system changes with increasing loop radius. The core radius is taken as $r_c = 20\,\text{Å}$[23] and the curves are plotted for wall widths $W = 10\,\mu\text{m}$ and $W = 3\,\mu\text{m}$, the values being those measured from micrographs of polymer orientated in a moderate (1 Tesla) field and a high (6 Tesla) field[5]. In both cases the energy passes through a maximum before decreasing with increasing loop radius, indicating that, once a loop of sufficient size has been nucleated within a wall, the loop will expand outwards, growing an area of undistorted liquid crystal within it and consuming the wall. For the wall width of $10\,\mu\text{m}$, a loop of approximately $20\,\mu\text{m}$ would have to nucleate before it would grow to destroy the wall. This is too large a size for nucleation to occur under usual circumstances, but as the wall width is decreased (i.e. as the field strength is increased) the necessary nucleation size becomes substantially smaller. The possibility of loops expanding to consume a wall may account for the apparent lack of domain walls in the samples treated under high fields[5]. Such calculations do not include the effect of the magnetic field explicitly, only in so much as to stabilize

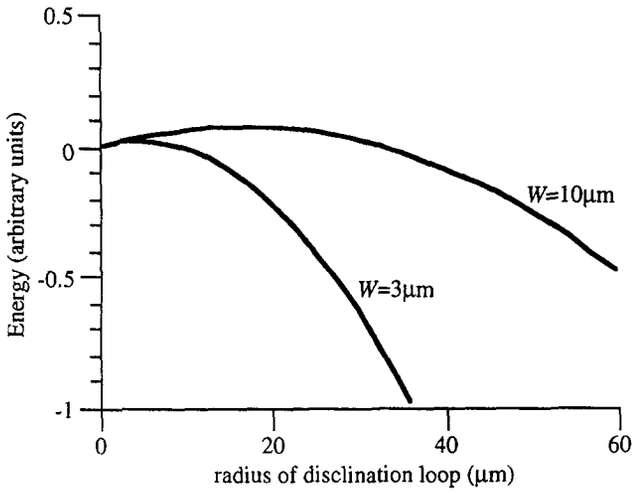

Figure 12 The variation in energy with loop radius for a disclination loop formed within a wall, calculated from equation (12) with wall widths $W = 10\,\mu\text{m}$ and $W = 3\,\mu\text{m}$

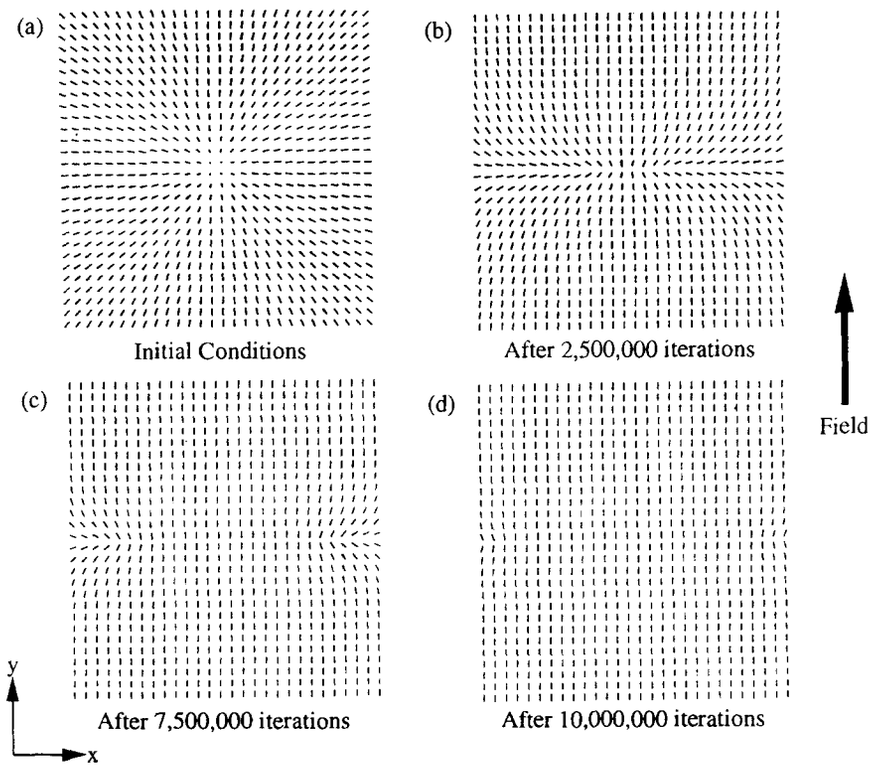

Figure 13 Model section through a 'hedgehog' point defect (a) under the influence of a field ($F = 0.2$). As the point relaxes (b–d), an $s = +1/2$ tangential loop is formed (i.e. one in which the rotation vector lies parallel to the line of the disclination right around the loop) which expands to enclose an area of well aligned directors. Eventually the loop is lost from the edge of the model

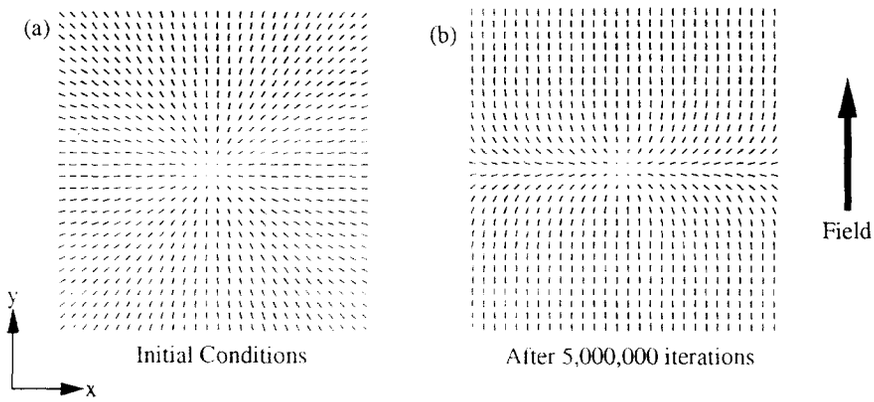

Figure 14 The relaxation under the influence of a field ($F = 0.2$) of a nematic containing a particle which aligns the local directors homeotropically to its surface. Initially (a), the particle imposes a radical vector field throughout the lattice: these are the starting conditions. As the field is applied (b), the defect is distorted to align more vectors to the field axis, but a loop is not formed to destroy the point. After this number of iterations, the texture has reached equilibrium: the vectors are no longer changing in orientation

the wall and to set the wall width. The expression for the energy of the disclination loop assumes an equilibrium director field around the disclination core when no field is applied.

Disclinations that pre-exist within a structure and are free to move are liable to do so to destroy domain walls. The influence of the field is such that it enhances the movement of disclinations with antiparallel rotation vectors (or 'opposite sign') towards one another, and eventually they annihilate. Thus it is the movement of disclinations, given sufficient mobility, that provide a key mechanism for the relaxation of textured nematics under the influence of the field.

POINT DISCLINATIONS

In the case of point defects in liquid crystals, the field will tend to break these points into disclination loops (of type II as defined in ref. 21) in which the rotation vector follows the loop around, the rotation vector (but not necessarily the line of the loop) lying in a plane perpendicular to the field direction. The loop forming at the centre of the point defect vector field will thus enclose an area of monodomain. For example, simulations of the relaxation of a hedgehog defect (one in which all directors radiate out from a central point) without a field indicate that it will not spontaneously decompose into a large disclination loop, but when a field is applied, the point splits into a loop in which the vector of rotation of the disclination is parallel to the tangent of the loop at all points around it. *Figure 13* shows this process with series of director maps of a single plane through the loop, showing the two points at which the loop cuts this plane. As the point relaxes, the disclination loop grows until it is lost from the edges of the model and a monodomain is formed, orientated in the field direction. If the starting structure were to contain point defects stabilized by second phase particles which encourage homeotropic alignment of the director to the particle surface, the defect may be stabilized even under magnetic alignment, the director field being distorted so as to increase alignment to the field. This effectively compresses the hedgehog into a cylindrically symmetrical wall normal to the applied field. The progression is shown in *Figure 14*: the 16 vectors at the centre of the lattice are fixed in their orientation to simulate the effect of a particle. On application of the field (*Figure 14b*), the point defect remains stable.

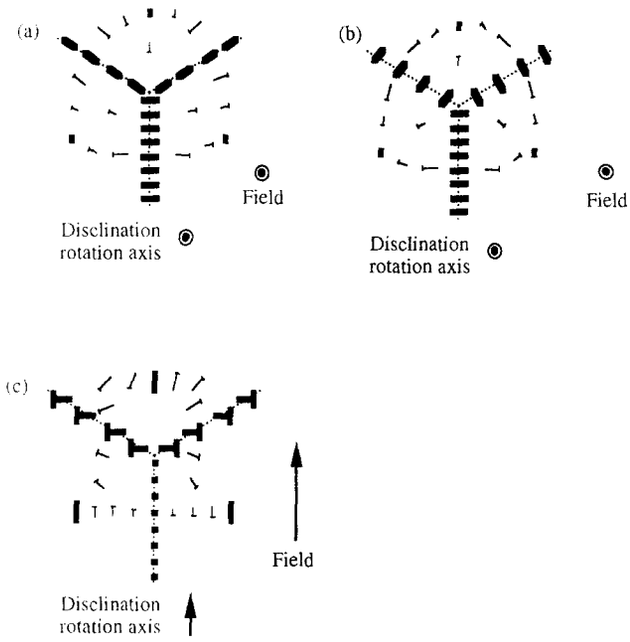

Figure 15 The junctions of three domain walls (dotted lines) and the director fields around them. Those vectors towards the centre of the domains must lie parallel to the field direction (shown in bold), and those at the very centre of the walls must lie perpendicular to the field direction (shown in bold). In each example there is disclination at the junction between the three walls with a rotation axis as indicated

JUNCTIONS BETWEEN DOMAIN WALLS

The domains that form on magnetic orientation have been observed to tessellate; the domains are defined by a continuous network of walls which meet along lines forming the junction between three walls. At a meeting point of three walls, a strength $\frac{1}{2}$ disclination is necessarily formed along the axis of intersection of the walls. Kléman illustrated this for the junction of three Bloch walls in magnetic materials[22], and Wood and Thomas[24] observed the inclusion of disclinations in domain walls in oriented thin films. Some examples of the line junctions of three walls with their associated disclinations are shown in *Figure 15*. The network of these triple wall lines in the domain structure may be thought of as a network of disclination lines, and the walls connecting them as the effect of the applied field on the director field around the disclinations. Consideration

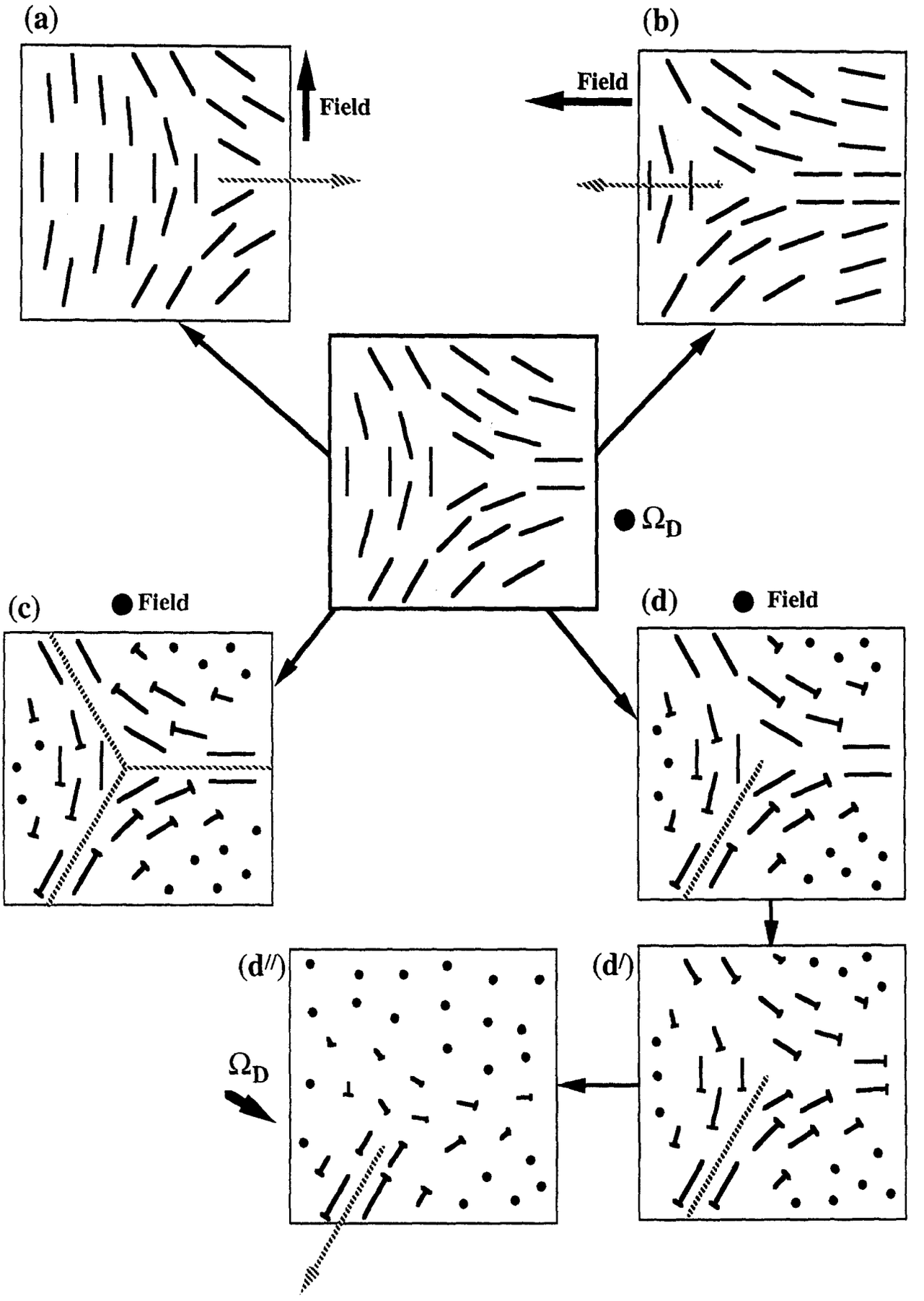

Figure 16 The action of a field on a disclination, in this case an $s = -1/2$ wedge, with rotation vector perpendicular to the page. If no field is applied (box with bold outline) the disclination would only move under the influence of other defects or surface interactions. (a) A field applied horizontally (perpendicular to Ω_D) mobilizes the disclination, forming a temporary wall (shown with a dashed line) and the disclination moves to the left, swallowing the wall. If the field is applied vertically (b) the mobilized disclination moves to the right. In (c) the field is applied parallel to Ω_D and the surrounding vectors orientate towards the field such that three walls are created. The resulting triple wall line is stable, and does not move. Another option when the field is applied parallel to Ω_D (d), is the formation of only one wall (d'). Ω_D rotates to lie perpendicular to the field (i.e. it becomes a twist disclination), and the disclination is mobilized to destroy the wall (d'').

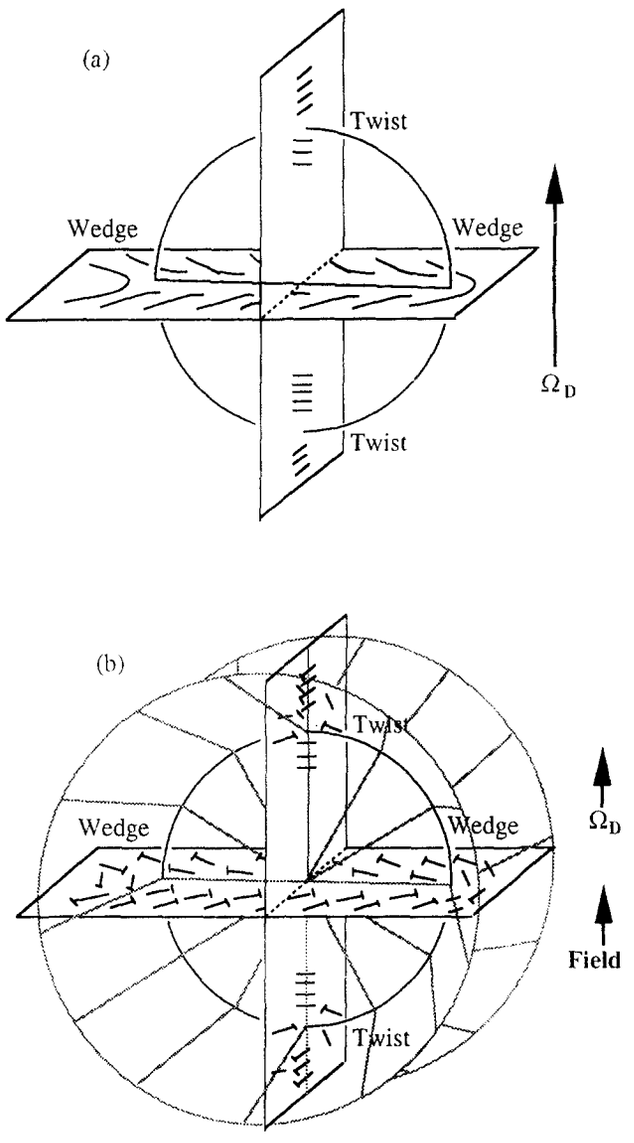

Figure 17 The action of a field on a loop of disclination with rotation axis parallel to the field. (a) The loop before the field is applied. The rotation axis of the disclination (Ω_D) lies in the plane of the loop, and so the character of the loop changes between wedge and twist as the loop is circled. On application of the field (b), if a triple wall is nucleated, it extends right around the loop, in this case forming a wall across the centre of the loop, and two truncated cones of wall extending away from the circle on either side of the loop. The walls are indicated by grey lines

of the effect of an applied field on a disclination (*Figure 16*) highlights the necessary factors required for a triple wall line to be stabilized. If no field is applied to the singularity (a $-\frac{1}{2}$ wedge line is chosen for this example), it is stable, and will only move in response to interactions with other disclinations, surfaces or external fields. This defect is shown in *Figure 16* in the box with the bold outline. If a field is applied perpendicular to the rotation vector of the disclination, the disclination is mobilized either to meet with other defects or to move out of the system (*Figures 16a* and *16b*). For a field applied parallel to the rotation vector, then it is possible for three walls to be established around the disclination core, and a stable triple wall line is formed (*Figure 16c*). Alternatively, if the surrounding vectors move in a different combination of directions towards the field (*Figure 16d*), then only one wall is formed. The other directors can then move towards the field direction (*Figure 16d'*), changing the rotation vector and hence mobilizing the disclination to leave a defect free area aligned to the field (*Figure 16d''*). Although this example has been given for a pure wedge disclination ($s = -\frac{1}{2}$ strength disclination) with its core running in the direction of the applied field, the result is general: the response of a disclination to an applied field is dependent only upon the relative directions of the disclination rotation vector and the field vector. On application of a field, each director surrounding a disclination rotates towards the field axis in the direction that is the shortest route towards the field axis; the vector will always rotate about an axis perpendicular to both the director being rotated and the field direction. Only when the director lies exactly perpendicular to the field direction are there two senses in which the director can move. This degeneracy is necessary for the formation of a triple wall line from a 'perfect' disclination (one in which, as illustrated in *Figure 16*, the director field away from the core always lies perfectly perpendicular to the rotation axis of the disclination), and so only in the special case of the disclination rotation axis lying parallel to the field direction can a triple wall line form. However, the director field away from the core of the disclination is not defined entirely by the topology of the singularity, and the elastic interactions with the surrounding director field will also influence the preferred direction of reorientation to the field. Thus, as the angle between the field and disclination rotation axes increases, the influence of the rotation axis to form a triple wall decreases, but the triple wall may still be formed as a result of elastic interactions from other directors in the neighbourhood. If the starting structure of the material is envisaged to consist of large areas of monodomain in random directions with defects between, a result of the powder from which the samples were made, then the response of the directors around the disclination will largely be a result of the orientation of these particles. Nevertheless, it is clear that a triple wall line which does form will have, along the junction line itself, a disclination with rotation vector parallel to the field axis.

The vector defining the direction of the disclination line determines only the wedge/twist character of the disclination and plays no part in the stability or otherwise of the walls that form on application of the field. This may be illustrated by consideration of the effect on a type I wedge/twist disclination loop of a field applied parallel to the single rotation axis defining the whole loop (*Figure 17a*). A triple wall line may be defined right around the disclination loop, forming a wall within the loop and two truncated cones of wall extending either side of the loop (*Figure 17b*).

Once a triple wall line has been nucleated in one region of a disclination, it will spread along its length. For a triple wall line to end, further defects must be included. The walls that form around a wedge-twist loop on application of a field parallel to Ω_D are shown in *Figure 17b*. These walls extend to infinity unless they meet another disclination which may bound them. Thus, once the wall network has been started, nearby disclinations will be 'dragged in' to form triple point junctions in order to minimize the wall area. Hence the tetrakaidecahedron structure is formed.

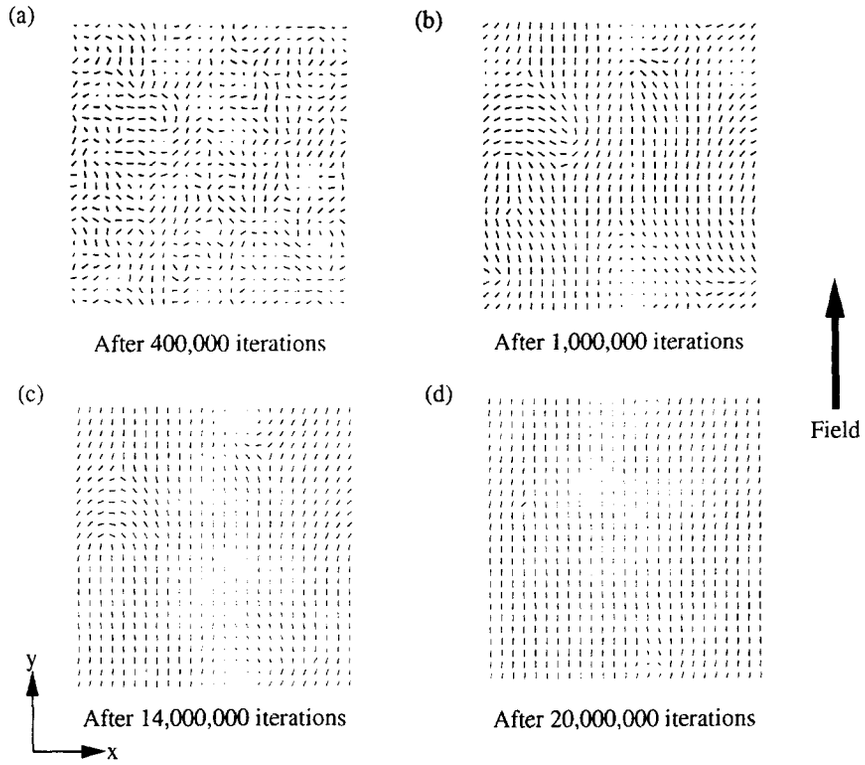

Figure 18 Director maps from a simulation with a starting condition of random directors (a) under the influence of an applied field ($F = 0.2$). (b) During relaxation walls begin to form, but they are bounded by disclinations of opposite sign (e.g. towards the left of the diagram) which move towards one another under the influence of the field (c) until eventually all defects are lost, and all vectors are aligned to the field direction (d)

FORMATION OF DOMAINS

If a lattice is set up with random vectors (*Figure 18a*), and its relaxation under the influence of a magnetic field simulated, the beginnings of wall formation may be observed (*Figure 18b*), but the walls are always bounded by disclinations which attract and annihilate (*Figure 18c*) until eventually a monodomain aligned in the field direction is formed (*Figure 18d*). A stable domain structure cannot be simulated from random starting conditions. It should be noted that the volume modelled (where a cell in the model is of the order of the diameter of the core of a disclination[21]) is very much smaller than that of any observed domain.

In practice, the polymer is not aligned from a completely random array of directors, but initially consists of local regions of quite well aligned polymer, which are not orientationally correlated to one another. Between these regions the liquid crystal contains many defects (points and/or disclinations). On application of the field to a sample, these well-ordered areas reorientate to the field direction and the areas of defects are compressed. The disclinations (any points present may be made into disclination loops by the action of the field) are mobilized, and annihilate; only some of those with the appropriate rotation vectors remain, and the walls between them result from the compression of the distortion around the disclination by the action of the field. The formation of a network of domains relies on an interlocking network of stabilized disclinations surrounding well-aligned regions. This may result from the particular starting microstructure of the material produced on melting a fine powder containing well aligned material. Note that the domain structure proposed above contains only disclinations with rotation vector parallel to the field direction.

An isolated domain in which the walls surrounding the aligned region did not enter triple wall lines would be unstable. Some of the walls on opposite sides of such a domain would necessarily be of opposite handedness, and therefore they would attract one another, decreasing the domain size and wall area until all the walls annihilate in a continuous process.

Once a network of domains is formed, the domains cannot shrink, and the observed domain structure is that resulting from the minimization of domain wall area.

Those walls which are at the 'top' and 'bottom' of the elongated domains are nearly perpendicular to the field direction and so contain principally splay/bend distortions. These will be of higher energy in polymer liquid crystals (which have a high splay elastic constant) than those down the longer 'sides' of the domains which lie parallel to the field and so can contain twist distortions. This minimization of splay distortions could account for the observed elongation of the domains along the field direction[5].

As many defects have been mobilized by the field to annihilate with one another during the orientation process, the orientated structure is on a larger scale than the untreated, but it still contains compressed defects (walls and disclinations) and so on removal of the field the orientation will be lost by the relaxation of elastic stresses in these defects, resulting in a coarser microstructure.

CONCLUSIONS

Under the influence of an applied field in an appropriate direction, an inversion wall will become narrower until an equilibrium width is reached. The width is inversely proportional to the field strength. The shape of

a splay/bend wall is determined by the ratio K_1/K_3. Measurements from orientated samples indicate that $K_1 > K_3$ for these materials.

An inversion wall may be described by a rotation vector in a similar way to a disclination. The direction of this rotation vector with respect to the wall plane normal determines the splay/bend or twist character of the wall, and it is the summation of these vectors which determines the interaction behaviour between walls or between walls and disclinations.

A disclination loop which encircles an area of wall within a monodomain will tend to collapse and annihilate, but a disclination loop within an area of wall which encircles well orientated material will grow to consume the wall if the loop radius is greater than a critical value. This radius is smaller for larger applied fields.

In general, a field acts to mobilize the disclinations by defining a direction in which they can move to increase the volume of material aligned parallel to the field. Thus the field acts to relax the structure, decreasing the overall number of disclinations. Disclinations whose rotation axis is parallel to the field are not mobilized by the field, however, and may form the junction between three domain walls.

A triple wall junction may be formed around a disclination if the directors around the core reorientate towards the field direction in the appropriate manner. The closer the field direction is to the rotation axis of the disclination, the more probable this would be, but it also depends upon the wider elastic interactions with the directors away from the core of the liquid crystal. A triple wall line, of any orientation, will have a disclination line at its core with rotation axis parallel to the field direction. Once a wall network is started by the formation of a triple wall junction, other disclinations will be dragged in to form the junctions between walls in order to minimize the overall wall area, and so the domain structure is formed.

The walls perpendicular to the field direction are necessarily of the splay/bend type, but those with the field axis in the plane of the wall may contain twist distortions. The observed elongation of the domains along the field direction may be accounted for by the reduction in splay distortion resulting from an increase in the relative area of the lower energy twist walls.

ACKNOWLEDGEMENTS

The authors would like to thank Hoechst-Celanese for providing materials used in this work, and SERC, ICI plc and the Cambridge Philosophical Society for funding.

REFERENCES

1 Anwer, A. and Windle, A. H. *Polymer* 1991, **32**, 103
2 Moore, R. C. and Denn, M. M. in 'High Modulus Polymers: Approaches to Design and Development' (Eds A. E. Zachariades and R. S. Porter), Marcel Dekker, New York, 1988
3 Assender, H. E. and Windle, A. H. *Polymer* 1996, **37**, 371
4 Assender, H. E. PhD Thesis, University of Cambridge, 1994
5 Anwer, A. and Windle, A. H. *Polymer* 1993, **34**, 3347
6 Windle, A. H. *Farad. Disc.* 1985, **185**, 186
7 Nehring, J. and Saupe, A. *J. Chem. Soc. Farad. Trans. II* 1972, **68**, 1
8 Thomson, W. *Acta Math.* 1887, **11**, 121
9 Plateau, J. 'Statique experimentale et theorique des liquides soumis aux seules forces moleculaires', Gauthier-Villars, Paris, 1873
10 Weaire, D. *New Scientist*, 1994, 21st May, 34
11 Ford, J. R., Bassett, D. C., Mitchell, G. R. and Ryan, T. G. *Mol. Cryst. Liq. Cryst.* 1990, **180B**, 233
12 Chandrasekhar, S. and Ranganath, G. S. *Adv. Phys.* 1984, **35**, 507
13 Noel, C., Monnerie, L., Achard, M. F., Hardouin, F., Sigaud, G. and Gasparoux, H. *Polymer* 1981, **22**, 578
14 Zheng-Min, S. and Kléman, M. *Mol. Cryst. Liq. Cryst.* 1984, **111**, 321
15 Meyer, R. B. in 'Polymer Liquid Crystals' (Eds W. R. Krigbaum, A. Ciferri and R. B. Meyer), Academic Press, New York, 1982
16 Lee, S-D. and Meyer, R. B. *Liquid Crystals* 1990, **7**, 15
17 de'Nève, T., Kléman, M. and Navard, P. *Liquid Crystals* 1995, **18**, 67
18 Bedford, S. E., Nicholson, T. M. and Windle, A. H. *Liquid Crystals* 1991, **10**, 63
19 Bedford, S. E. and Windle, A. H. *Liquid Crystals* 1993, **15**, 31
20 Assender, H. E. and Windle, A. H. *Macromolecules* 1994, **27**, 3439
21 Windle, A. H., Assender, H. E. and Lavine, M. S. *Phil. Trans. Royal Soc. London* 1994, **347**, 73
22 Kléman, M. 'Points, Lines and Walls', Wiley, Chichester, 1983
23 Cladis, P. E. *Phil. Mag.* 1974, **29**, 641
24 Wood, B. A. and Thomas, E. L. *Nature* 1986, **324**, 655